

Crystal structure refinements of palygorskite and Maya Blue from molecular modelling and powder synchrotron diffraction

GIACOMO CHIARI^{1*}, ROBERTO GIUSTETTO¹ and GABRIELE RICCHIARDI²

¹Dip. di Scienze Mineralogiche e Petrologiche, Università di Torino, Italy Via Valperga Caluso 35, I-10125 Torino, Italy

*Corresponding author, e-mail: giacomo.chiari@unito.it, robgiust@dsmp.unito.it

²Dip. di Chimica IFM, Università di Torino, Via Pietro Giuria 7, I-10125 Torino, Italy
e-mail: gabriele.ricchiardi@unito.it

Abstract: Maya Blue, a synthetic pigment produced by the ancient Mayas, is a combination of a specific clay, palygorskite (or sepiolite), containing large channels in the crystal structure and the organic dye indigo. Little is known about the interaction of the two components to give the most stable pigment ever produced. The aim of this work is to obtain a refined model for the Mexican palygorskite used to prepare the pigment and to elucidate the structure of the clay-indigo complex, using both molecular modelling and Rietveld refinement on data collected with synchrotron radiation. Molecular modelling proved that indigo can fit into the channels without steric impediment (forming strong hydrogen bonds between the C=O group of the dye and the structural water of the clay) and produced a model, showing reasonable distances and angles, used as the starting set for the Rietveld refinement. Difference Fourier maps, calculated without indigo, showed a residual of electron density coherent with the expected disordered position of the indigo molecule. A refinement carried out using the model of palygorskite obtained in this work and a 6-fold disordered arrangement of indigo confirmed these findings. The ratio between the two polymorphs of palygorskite (monoclinic and orthorhombic) present in the natural clay was obtained for our sample and for several palygorskite specimens coming from different sites. Samples within the same outcrop show similar ratios, while samples from different locations do not. This may be used to characterize the provenance of ancient specimens, with the goal of determining whether Maya Blue was invented and produced in one place only or if the production technology was widespread in all the Mayan region.

Key-words: Maya Blue structure, palygorskite structure, synchrotron powder refinement, indigo.

1. Introduction

Maya Blue (MB hereafter) is a characteristic pigment, produced by the Mayas probably around the VIII century AD. Its colour can show various hues, ranging from a bright turquoise to a dark greenish blue. Due to its beauty, it was used (mostly in Mexico but also in Cuba, Tagle *et al.*, 1990) in mural paintings, statues, ceramics, codices, and even to paint prisoners to be sacrificed (Reyes-Valerio, 1993). The Maya civilization was “discovered” in modern times in the middle of the last century, by Stephens and Catherwood (Stephens, 1841; Catherwood, 1844). Since then, tremendous progress has been made from the archaeological point of view, in understanding the way of life as well as the technologies used by the Mayas (see *e.g.* Sharer, 1994).

MB is extremely stable: it can resist the attack of boiling, concentrated nitric acid, alkali and any sort of organic solvents. In spite of being the subject of several studies, its composition remained a mystery for a long time (Merwin, 1931; Gettens & Stout, 1942, who gave Maya Blue its name; Shepard & Gottlieb, 1962; Magaloni, 1998). Roundhill *et al.* (1989) summarized this endeavour well. Towards the

end of the '50s, X-Ray Powder Diffraction analysis showed that the pigment contained the clay mineral palygorskite, then called attapulgitite. Gettens (1962) first proposed that the blue colour of the pigment was due to the presence of indigo. Littmann (1980) thought that the pigment was a naturally blue montmorillonite but later (1982) acknowledged the validity of the palygorskite/indigo complex theory. Cabrera (1969) studied original samples while Van Olphen (1966) and Kleber *et al.* (1967) were able to recreate an artificial pigment presenting the same blue colour and stability as MB, by mixing indigo and palygorskite and heating the mixture to ~150 °C for 20 hours, thus discovering the fundamental role played by heat in the pigment manufacture. By merely mixing palygorskite and indigo the resulting compound, although similar in aspect to MB, was not resistant to chemical attack.

Indigo was utilized as a dye in India, in ancient Egypt, in China, by the Greeks and the Romans. In the New World indigo was used to dye fabric and to colour the face and bodies in pre-Cortez times. In Peru it was used for textiles in Paracas (Fester, 1955). The Mayas extracted it from the leaves of *Indigofera suffruticosa*, a native American plant which is a

close relative to the *Indigofera tinctoria*, typical of the Far East (Reyes Valerio, 1993; Torres Montes *et al.*, 1975).

Several hypotheses were presented on how MB was produced using only the relatively crude technology at the Mayas disposal. Reyes-Valerio (1993) perfected the pigment preparation procedure, using techniques presumably adopted by the ancient Mayas. He produced a pigment very similar to the ancient one, by mixing palygorskite and *Indigofera suffruticosa* leaves in water, oxidising the suspension and heating the filtered mixture at $\sim 100^\circ\text{C}$ for 30 to 60 minutes. We repeated the preparation with success, but heated it for a longer period of time (from 12 to 24 hours. Actually the timing is not an important issue in the preparation, provided that the mix is let to dry well). A sample prepared by Reyes-Valerio was used for the data collection in this study.

IR spectroscopy (Kleber *et al.*, 1967; Palacios-Lazcano & Reyes-Valerio, 1993) and recently photoluminescence spectroscopy (Ajò *et al.*, 2000) unequivocally revealed the presence of indigo in both the antique pigment and in the synthetic one, since both show almost identical patterns.

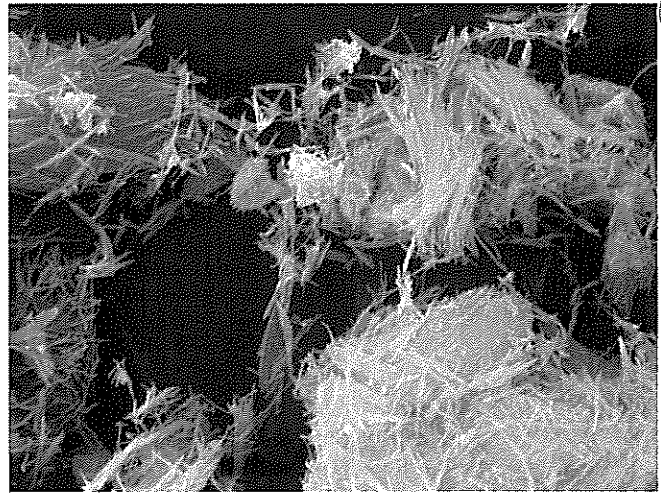
Therefore it was proven that it is not only possible, but actually rather easy to manufacture the pigment. The preparation works equally well with industrial synthetic indigo. However, despite great effort the structural details of the clay-indigo complex are not known.

The inorganic part is made of palygorskite and sometimes sepiolite (if we do not consider kalifersite, (Ferraris *et al.*, 1998), which is a member of the palygorskite/sepiolite polysomatic series, having a channel of palygorskite alternating with a channel of sepiolite). Brindley (1959) was able to index the pattern and determine the space group of sepiolite, while its crystal structure, proposed in general terms by Brauner & Preisinger (1956), has never been refined.

According to Kukovskiy & Ostrovskaya (1961), the name "palygorskite" was used to identify a mineral discovered in 1860 in a mine at Palygorsk (ex USSR). The same mineral found at the site of Attapulgis (Georgia, USA) was named "attapulgitite" by De Lapparent (1938). In 1985 the IMA commission for Mineral nomenclature definitely approved the name palygorskite for the clay, although many people (for example the art conservators) still use the name attapulgitite to indicate the material used for cleaning poultices. The first structural model for palygorskite was proposed by Bradley (1940) and reviewed by Preisinger (1963), but the tools to carry out a refinement of such a complex structure (necessarily using powder diffraction data since there are no single crystals of sufficient magnitude – see Fig. 1), were simply not available at the time. Chisholm (1990, 1992) reviewed the structural model of palygorskite, without refining the atomic coordinates. He distinguished two polymorphs (orthorhombic and monoclinic). Artioli & Galli (1994) using a conventional powder X-ray diffractometer, and Artioli *et al.* (1994) and Perego (1998), using synchrotron radiation, carried out a full refinement of the model.

Palygorskite has been used for the production of ceramic in the Chapas region (Mexico) for the last 800 years, according to Singer & Galan, (1984). Fig. 1 shows the fibrous clay as seen by ESEM (Environmental Scanning Electron microscope).

Goal of the present study is to determine the structure of the complex and to use this information to understand its



6µm 4000X

Fig. 1. Environmental Scanning Electron Microscope picture of palygorskite. (Photo: Eric Doehne, Getty Conservation Institute).

preparation more in detail. This is important from the archaeological point of view, since it is still unknown whether the Mayas made use of a specific clay, coming from a well defined deposit (knowing that only with that type of clay the pigment could be produced) or if the clay was simply contained in the water, without the manufacturers of the pigment even noticing it. Moreover, it is unknown whether MB was discovered and produced in one single place and sold to all other Mayan cities, or if the technology was exported and each town was able to produce its own MB. The knowledge of the relative abundance of the two polytypes of palygorskite in the clay may be of help in solving the provenance problem (Chiari *et al.*, 2000). In fact, if samples of MB coming from different places have different monoclinic/orthorhombic ratios, the local production may be favoured. If the ratio is constant independently from the location of the pigment, the hypothesis of a single production site seems more likely.

2. Description of the precursors of Maya Blue

Palygorskite is a dioctahedral clay, with fibrous morphology and ideal composition $(\text{Mg, Al})_4\text{Si}_8(\text{O, OH, H}_2\text{O})_{24} \cdot n\text{H}_2\text{O}$. Normally it is a mixture of two different polytypes: one monoclinic (space group $C2/m$ – MP hereafter) and one orthorhombic (space group $Pbmn$ – OP hereafter) (Chisholm, 1992). Both polytypes show discontinuous octahedral layers, forming ribbons elongated in the Z-axis direction. The tetrahedral layers present regular inversions of the orientation of the SiO_4 tetrahedra apexes, occurring every two chains. Palygorskite is therefore crossed by zeolitic-like channels along Z, usually occupied by weakly bound, non-structural water (zeolitic water). Mg and Al cations complete their co-ordination with tightly bound water molecules (structural water) (see Fig. 2).

Indigo (see Fig. 3) was first synthesized in 1880 by Von Bayer, after 15 years of intense studies. Only in 1897 was

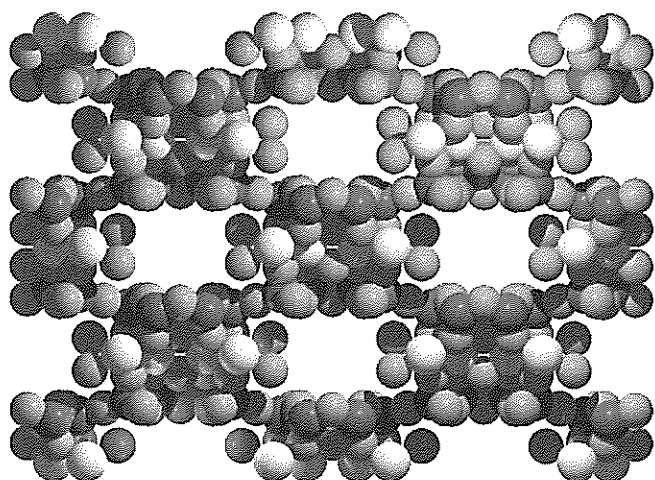


Fig. 2. Structure of palygorskite projected on the (001) face. The zeolitic water molecules were removed, showing the empty channels, whose dimensions are $7.3 \times 6.3 \text{ \AA}$. (Graphic programs: MOLDRAW & POV-RAY)

the first synthetic indigo commercialised. As a consequence, the huge plantations of *Indigofera* plants have mostly been destroyed (Virno, 1986).

According to the most quoted hypothesis on MB structure, the indigo molecules can be accommodated inside the palygorskite channels and form chemical bonds with the clay, thus explaining the pigment's strong stability. Thermogravimetric (TGA) and Differential Thermal (DTG) analysis carried out on palygorskite (Artioli *et al.*, 1994) showed that by heating the clay up to $300 \text{ }^\circ\text{C}$ the zeolitic water is progressively lost, emptying portions of the channels. This loss may allow for the entry of indigo molecules, whose dimensions are compatible with those of the clay channels (indigo molecule approximately 4.8 \AA wide; palygorskite channels: 7.3 \AA , sepiolite channels: 13.7 \AA in width).

It is very likely that the indigo molecules are not randomly distributed along the clay channels. The formation of hydrogen bonds between the hydroxyl groups of the clay and the C=O group of indigo requires the indigo molecules to have a precise position inside the clay structure. If so, indigo can affect both the symmetry and lattice periodicity of MB, which may be considered as a palygorskite/indigo complex, having a proper crystal structure, although not perfectly ordered.

Molecular modelling on MB have recently been attempted, using CERIU2 program (Polette *et al.*, 2000), although no detailed results were given. In order to test the encapsulation of the indigo, molecule into the framework of orthorhombic and monoclinic palygorskite, molecular modelling techniques were used. The aims were to predict the location of indigo and to analyze the steric, dispersive and hydrogen bond interactions between the dye molecule and the clay framework. In fact, these H-bonds may be responsible for the remarkable stability of the pigment. The possibility of displacement of adsorbed water by indigo was also taken into account, because of its implications in the synthesis of MB.

A Rietveld refinement was first carried out on the Mexican clay used for the preparation of synthetic MB, in order

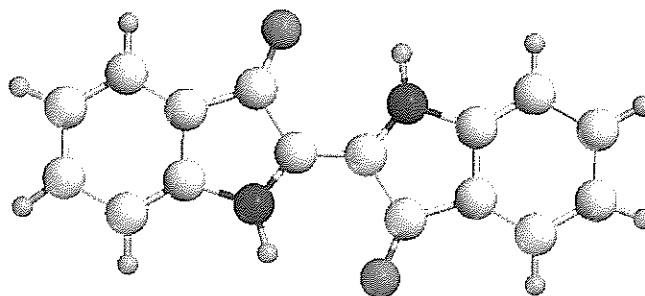


Fig. 3. The indigo molecule. Its dimensions are such ($4.8 \times 12.3 \text{ \AA}$) that it can fit well inside the palygorskite channels.

to have a good structural model. In fact, minor differences could exist between the structure of palygorskite from Mexico (Sac lu'm) and the structural models reported in the literature.

Subsequently, a Rietveld refinement was carried out on synthetic MB to identify the changes introduced by the presence of indigo.

3. Experimental

The samples of palygorskite used for the MB preparation in this work came from the mine of Lorenzo Pech, a few kilometres from Ticul on the road to Chapab (Chapas) (Audagnotti, 2001). For both palygorskite and Maya Blue, powder diffraction data were collected at the D8 GILDA beam line (General Italian Line for Diffraction and Absorption) at the European Synchrotron Radiation Facility (ESRF) in Grenoble, France, by Gilberto Artioli. The bending magnet beam line optics encompasses a double crystal Si monochromator, with the second crystal sagittally bent to focus the beam in the horizontal plane, and a vertically focusing Pt coated mirror (Pascarelli *et al.*, 1996). A wavelength of $0.82648(2) \text{ \AA}$ was selected for the experiment and calibrated against the reference silicon sample (NBS 640b, having a $= 5.430954 \text{ \AA}$ at $26 \text{ }^\circ\text{C}$). The samples were hand ground, loaded into a 0.3 mm diameter Lindemann capillary, and attached on a standard goniometer head. The latter was mounted on the ϕ axis of a two-circle diffractometer and axially rotated during the data collection in Debye-Scherrer geometry. The whole diffraction rings were recorded on an Fuji Image Plate located at 25.5 cm from the sample, and perpendicular to the incident beam. The sample to detector distance and residual tilt angles were calibrated by analysis of the diffraction data obtained on standard Si and LaB_6 samples (NBS/NIST 640b and 660a, respectively) in the same experimental conditions. All calibrations and data processing were performed on the scanned digital images (Fuji BAS2000 Scanner) by using the Fit2d program package (Hammersley *et al.*, 1996). The diffraction rings were radially integrated, and the intensities corrected for flat plate geometrical distortion and polarisation (polarization factor $= 0.96$), thus eliminating errors due to preferred orientation of the crystallites. Since the clay is fibrous, this effect, without the above correction, could have been a serious bias in the data collection. The intensity data were then interpolated

Table 1. Comparison between Rietveld refinements of Sac lu'm (Mexican palygorskite) and Maya Blue. a) Formula, space group, cell parameters, and refinement data. b) Data collection description and agreement factors. c) Refined atomic coordinates for MP and OP in palygorskite, and in the "1-cell disordered" model of Maya Blue.

Table 1. a

	MP	OP	MP+indigo	OP+indigo
Formula	(Mg, Al) ₄ Si ₈ (O, OH, H ₂ O) ₂₄ •nH ₂ O		(Mg, Al) ₄ Si ₈ (O, OH, H ₂ O) ₂₄ •nH ₂ O + C ₆ N ₂ O ₂	
Space group	<i>C2/m</i>	<i>Pbmn</i>	<i>C2/m</i>	<i>Pbmn</i>
<i>a</i> (Å)	13.304(4)	12.762(3)	13.380(3)	12.720(3)
<i>b</i> "	17.876 (7)	17.882(4)	17.885(4)	17.886(3)
<i>c</i> "	5.251 (2)	5.249(1)	5.250(1)	5.254(1)
β(°)	107.01 (3)	-	106.81(2)	-
<i>V</i> (Å ³)	1194.1 (6)	1197.9(4)	1202.6(3)	1195.4(3)
Weight frac. (%)	52.8 (8)	35.5(7)	47.3(5)	40.6(5)
Δρ _{min} , Δρ _{max} (e/Å ³)	-0.56, 0.75	-0.92, 1.00	-0.56, 0.51	-0.57, 0.62
GW, L(X)	5(1), 15.2(7)	5(1), 15.2(7)	0.6(8), 1.6(7)	0.6(8), 1.6(7)

Table 1. b

Diffractometer	D8 GILDA beamline, ESRF-GrènoBLE (France)		
λ, T (K)	0.82648(2), room temperature		
Detector distance (cm)	25.5		
Rotation axis	φ		
2θ max (°)	50		
	palygorskite	Maya Blue (3-cells)	Maya Blue (1-cell)
R	4.74	2.89	2.45
R _{wp}	6.33	4.07	3.40
χ ²	35.07	18.47	14.72

to fixed angular steps, and converted into a conventional diffracted intensity vs. diffraction angle profile.

The GSAS program package (Larson & Von Dreele, 1986) was used for all Rietveld refinements.

4. The refinement of the Mexican palygorskite (Sac lu'm)

A small amount of calcite was present in the veins of the clay outcrop (Audagnotti, 2001). The details of the data collection are resumed in Table 1b. The lattice parameters and atomic coordinates for MP were taken from Artioli & Galli (1994), for OP from Chisholm (1992) and for calcite from Effenberg *et al.* (1981). The refinement conditions, agreement factors, cell parameters, weight percentages and atom coordinates of both palygorskite polymorphs are reported in Tables 1(a, b and c).

In the early stages of the refinement only the scale factors, the lattice parameters and the profile coefficients for each phase were adjusted. Subsequently, the atomic coordinates and the occupancy factors for all atoms were refined. Soft constraints on tetrahedral and octahedral bond lengths and angles were imposed, and structurally related parameters were allowed to vary in alternate cycles, to avoid possi-

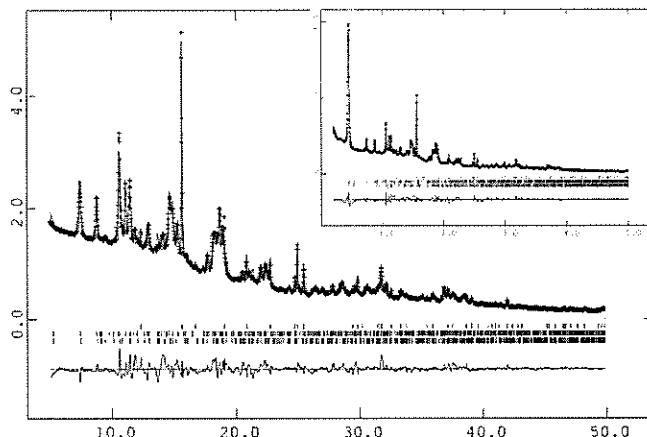


Fig. 4. Rietveld refinement profile of Sac lu'm, the Mexican palygorskite used to prepare the synthetic Maya Blue.

ble correlations. In the final stages, the overall isotropic thermal parameters for each chemical species were also refined. Fig. 4 shows the *observed*, *calculated* and *difference* powder diffraction patterns for the Sac lu'm sample.

Difference Fourier maps for both palygorskite polymorphs showed reasonably low electron density residues (Table 1a). The refinement showed no appreciable improvement by adopting a trioctahedral model for the orthorhombic polymorph, as proposed by Preisinger (1963). The occupancy factor of a Mg cation, placed at 0,0,0 decreased to zero, confirming the dioctahedral nature of the clay, in accordance with recent chemical analysis (Artioli *et al.*, 1994).

A comparison between these models and the ones present in the literature (Artioli & Galli, 1994 and Chisholm, 1992) was made, by calculating the shifts between homologous atoms. The refined model proved to be coherent with the above quoted structures. The average difference between corresponding atomic positions (excluding the zeolitic water) was 0.35 and 0.26 Å (for the orthorhombic) and 0.1 and 0.53 Å (for the monoclinic structures) between our refinement and the ones by Artioli & Galli (1994) and Chisholm (1992) respectively. It should be pointed out that the

Table 1. c

Palygorskite MP					OP			
Atom	x	y	z	Frac.	x	y	z	Frac.
Si1	0.185(1)	0.0817(6)	0.069(4)	1.00	0.240(1)	0.0848(6)	0.809(3)	1.00
Si2	0.209(1)	0.1673(4)	0.587(3)	1.00	0.2059(9)	0.1667(5)	0.326(3)	1.00
Mg2	0	0.086(2)	0.5	1.00	0	0.084(2)	0.5	1.00
Mg3	0	0.207(2)	0	1.00	0	0.148(2)	0	1.00
OH	0.092(3)	0	0.52(1)	1.00	0.076(3)	0	0.288(8)	1.00
O1	0.069(2)	0.099(2)	0.117(5)	1.00	0.113(1)	0.091(1)	0.780(4)	1.00
O2	0.092(2)	0.174(1)	0.640(5)	1.00	0.079(1)	0.164(1)	0.321(4)	1.00
W1	0.078(4)	0.312(2)	-0.04(1)	1.00	0.086(3)	0.238(2)	0.856(7)	1.00
O3	0.225(3)	0	0.006(6)	1.00	0.275(2)	0	0.852(6)	1.00
O4	0.25	0.25	0.5	1.00	0.25	0.25	0.378(5)	1.00
O5	0.238(2)	0.106(1)	0.383(5)	1.00	0.268(1)	0.118(1)	0.533(3)	1.00
O6	0.247(2)	0.126(1)	0.882(4)	1.00	0.219(2)	0.140(1)	0.041(3)	1.00
ZW1	0	0.349(2)	0.5	1.00	0	0.406(6)	0.5	1.00
ZW2	0	0.421(2)	0	1.00	0	0.4278(9)	0	1.00
Maya Blue MP + indigo					OP + indigo			
Atom	x	y	z	Frac.	x	y	z	Frac.
Si1	0.213(2)	0.099(2)	0.076(5)	1.00	0.221(1)	0.0824(9)	0.787(3)	1.00
Si2	0.215(2)	0.1733(8)	0.633(5)	1.00	0.205(1)	0.1657(9)	0.326(4)	1.00
Mg2	0	0.086(2)	0.5	1.00	0	0.093(2)	0.5	1.00
Mg3	0	0.156(3)	0	1.00	0	0.170(2)	0	1.00
OH	0.085(4)	0	0.44(1)	1.00	0.029(3)	0	0.278(8)	1.00
O1	0.091(2)	0.080(2)	-0.082(5)	1.00	0.094(2)	0.092(1)	0.807(5)	1.00
O2	0.098(2)	0.168(2)	0.679(5)	1.00	0.076(1)	0.156(2)	0.334(8)	1.00
W1	0.077(2)	0.248(1)	0.055(4)	1.00	0.110(2)	0.238(1)	0.780(7)	1.00
O3	0.163(4)	0	0.00(1)	1.00	0.204(4)	0	0.919(7)	1.00
O4	0.25	0.25	0.5	1.00	0.25	0.25	0.232(9)	1.00
O5	0.223(3)	0.117(2)	0.391(5)	1.00	0.274(2)	0.111(2)	0.516(5)	1.00
O6	0.288(2)	0.135(2)	0.908(5)	1.00	0.219(3)	0.129(2)	0.054(5)	1.00
ZW1	0	0.348(2)	0.5	0.74(3)	0	0.369(2)	0.5	0.65(3)
ZW2	0	0.395(2)	0	0.74(3)	0	0.5	0	0.65(3)
C1	0	0.5	0.3634	0.09(1)	0	0.5	0.3633	0.11(1)
C2	0	0.5776	0.2015	0.044(5)	0	0.5747	0.1905	0.056(6)
C3	0	0.5465	0.0625	0.09(1)	0	0.5437	0.0631	0.11(1)
C4	0	0.5835	0.3017	0.09(1)	0	0.5806	0.3027	0.11(1)
C5	0	0.5404	0.5233	0.09(1)	0	0.5376	0.5245	0.11(1)
N1	0	0.4394	0.2018	0.044(5)	0	0.4366	0.2015	0.056(6)
Oin	0	0.6444	0.2633	0.044(5)	0	0.6414	0.2631	0.056(6)

OP model proposed by Artioli & Galli (1994) contained two more atoms (one Mg and one O), which were not considered in our model. The Si-O bonds centred on O4, relative to the tetrahedra pointing the apices in opposite directions, are quite elongated (1.68 Å) in both polymorphs, indicating the presence of strong tension in the structure, and suggesting that the most likely cleavage should occur according to (100).

5. Molecular modelling

5.1. Calculation method and models

The energies and forces used in our simulations were calculated with molecular mechanics using the "cvff_aug" force-field from MSI (Molecular Simulations Inc., 1996). This forcefield includes an accurate set of diagonal and cross

terms for the organic molecule, while the clay framework is described with Coulomb and Buckingham potentials. Net formal charges of the ions were used, and all electrostatic interactions were calculated on periodic models with the Ewald method (Ewald, 1921).

Structure optimisations were obtained by minimizing the lattice energy of the models as a function of atomic coordinates and cell parameters, until zero-force structures were obtained. All optimisations were performed using the Discover 3.0 program from Molecular Simulations Inc. (1996). In order to avoid local energy minima, several minimizations were carried out, starting from different initial geometries. In water-containing models, the problem of the initial position of the water molecules was solved by manual addition of the hydrogen atoms close to the crystallographic position of the oxygen atoms. The final hydrogen positions were extracted from MD simulations using the same program, with a run at 300 K (parameters used: 100 picosec-

onds, 1 femtosecond time step, NPT ensemble with velocity scaling). This procedure generated structures to be used as starting sets for the Rietveld refinement, with randomly oriented water molecules forming hydrogen bonds with correct distances and angles. For all simulations, no symmetry constraints were imposed.

For models regarding palygorskite alone, without indigo, a single-cell periodic structure was used, while the introduction of indigo required the use of $1 \times 1 \times 3$ periodic super-cells (triple along the Z axis). This was done because one cannot be sure a priori that indigo is completely disordered.

For the MD simulation, periodic models of monoclinic and orthorhombic palygorskite were constructed, starting from the structures proposed by Chisholm (1992), and by Artioli & Galli (1994), including the oxygen atom of the structural water molecules. Hydrogen atoms were added manually and their position was refined using the above described MD methods. The final optimised structure was not dependent upon the initial structure. Since the orthorhombic and monoclinic models of the structure proposed by Chisholm (1992) have the same connectivity, the possibility of the inter-conversion between the two polymorphs has also been investigated. Initial structures were generated by manually deforming the cell parameters to mimic the ones observed in the other polymorph, and keeping the atomic fractional coordinates unchanged. Geometry optimisation was then run on these models. In all cases, optimisations reproduced the original undistorted structures. This indicates that the inter-conversion between the two polymorphs cannot take place by thermal motion or weak mechanical constraints, as observed, for example, in some zeolite structures (Van Koningsveld *et al.*, 1987).

A reasonable Maya Blue model starting from the “non-classical” orthorhombic structure proposed by Artioli & Galli (1994) could not be assembled, because the presence of dangling Si-OH groups into the channels precluded the presence of indigo for steric reasons.

Al^{3+} and Mg^{2+} ions occupied the octahedral layer with a 1:1 ratio, giving a neutral framework, without the need for extra-framework cations. In a few trials, zeolitic water molecules and indigo were simultaneously present.

The symmetry operators of both parts were maintained and combined as much as possible, thus postulating a MB structure with maximum symmetry. The flat indigo molecule lies parallel to the (100) plane of palygorskite, with its major axis oriented along the channel. The symmetry centre of indigo (located at the middle of the C=C double bond) coincides with the clay symmetry centre located at $c/2$. This choice allows for the conservation of symmetry operators for both precursors: the mirror plane, normal to the Y axis in the clay lattice, divides the indigo molecule (along the major axis) in two halves, which appear to be enantiomorph if one considers the N-H and C=O groups to be interchangeable. This is necessarily so for disorder reasons (see below).

The length of the indigo molecule and of c parameter of the clay suggests the formation of a 3-cells superstructure (a , b , 3^*c). The symmetry for the proposed 3-cells superstructures maintain the space groups for both the monoclinic ($C2/m$) and the orthorhombic ($Pbmm$) palygorskite. Two indigo molecules are present in each super-cell.

The idea of a $\approx 16 \text{ \AA}$ long super-lattice in the MB structure was previously proposed by Yacaman & Serra Puche (1995), based on HRTEM image processing. The super-lattice existence was supposed to be caused by the indigo insertion in the clay channels, although no further details were given.

The following models were calculated:

a) monoclinic (MP) and orthorhombic (OP) palygorskite with zeolitic water, representative of the structure of hydrated palygorskite.

P and OP in absence of zeolitic water, but with structural water, representative of the structure of the clay dehydrated at temperatures $> 300 \text{ }^\circ\text{C}$.

c) MP and OP palygorskite containing two indigo molecules for each triple super-cell, *i.e.* with the maximum indigo loading allowed by the structure.

For each of these models, a set of optimised coordinates and the lattice energies were obtained, which allowed for the evaluation of the adsorption enthalpy of indigo and water.

5.2. Calculation results

The adsorption of indigo on dehydrated palygorskite is predicted to be exothermic with adsorption enthalpies of -37 and -36 kJ/mol per indigo molecule for MP and OP structures respectively. This negative enthalpy results from a positive deformation energy of the clay (30 kJ/mol for both) counterbalanced by strong electrostatic and dispersive interaction (-65 and -63 kcal/mol). The deformation energy of the indigo molecule upon adsorption is found to be negligible (2 kJ/mol for both).

On the contrary, the adsorption of indigo on hydrated MP and OP is strongly endothermic (152 and 145 kJ/mol per molecule respectively), *i.e.* the clay has a strong preference for water as compared to the organic dye.

The difference between the adsorption energy of the MP and OP polymorphs is negligible (1 kJ/mol) for the dehydrated structure, and small (8 kJ/mol) for the hydrated structures. This is due to the higher hydrophilic character of the monoclinic structure (water adsorption energies calculated but not reported).

In all optimised structures the indigo molecule lies approximately in the middle of the channels, with the centre of the molecule on the centre of the triple super-cell. Minor distortions of the indigo molecule were observed, dictated by the steric constraints imposed by the randomly orientated structural water molecules. The C=O groups of indigo form hydrogen bond interactions with structural water, while no similar interactions were observed for the N-H groups. The optimised distances are 1.74(4) for OH-O and 2.62(1) for O-O in MP, and 1.85(1) for OH-O and 2.67(1) for O-O in OP. These values represent the average of four independent H-bonds. In OP the longer bond distances may be due to the fact that the channels are wider.

On the basis of the above results one can draw the following conclusions:

a) the introduction of indigo into the OP and MP channels is sterically possible. The space created by removing zeolitic water alone is sufficient to host the organic guest. The ad-

sorbed molecules are in close contact with the clay, but no unreasonably short bond distances were detected. Indigo spanned approximately three unit cells of palygorskite. The C=O groups of indigo can form short hydrogen bonds with the structural water of the clay.

b) the adsorption of indigo is energetically disfavoured as compared with the adsorption of water. This explains why heating above 100 °C is necessary in order to obtain the stable pigment. Indigo cannot displace water, but it can substitute it once that water molecules are driven away by thermal motion.

c) in agreement with the occupancies obtained from the refinement of the Maya Blue structure (see below), we observe that the displacement of water is slightly favoured for the orthorhombic structure.

As a whole, these results strongly support the hypothesis that indigo is stabilized by irreversible encapsulation into the clay structure, and that the insertion is due to high temperature diffusion, after the zeolitic water has emptied the cavities.

In all theoretical calculations the indigo molecule was inserted in the clay structure, respecting the dimensions of both the channel and the dye and optimising distances and angles.

Apart from these results, the chemical modelling also produced an optimised set of coordinates to be submitted to the XRPD refinement. The optimised coordinates (space group *P1*), which refers to a 3-cells superstructure since the indigo molecule length roughly corresponds to three times *c*, were transformed by averaging the corresponding atoms to obtain the symmetric set (space group *C2/m* for MP and *Pbmn* for OP).

6. Rietveld refinement of Maya Blue

To test the reliability of the MB structure obtained by the molecular mechanics simulations, a Rietveld refinement was carried out on a non-archaeological MB specimen, kindly provided by Constantino Reyes-Valerio and prepared using the same Mexican palygorskite (Sac lu'm) used for the refinement of palygorskite. The choice of a synthetic rather than an original MB sample was made in order to eliminate the interference from the support which cannot be eliminated from the specimens of ancient MB, and to have the same clay already refined as host framework.

A preliminary analysis of the collected pattern revealed the presence of small quantities of calcite and quartz. The starting model included therefore MP and OP palygorskite, encapsulating the indigo molecule, quartz and calcite. The data were taken from Glinnemann *et al.* (1992) for quartz and from Effenberg *et al.* (1981) for calcite.

The data were measured in the range $5^\circ \leq 2\theta \leq 50^\circ$, using $\lambda = 0.82648(2) \text{ \AA}$, since no peaks were located at higher 2θ values. Moreover, the strongest palygorskite peak located at approximately $2\theta = 2^\circ$ was excluded from the dataset, since it was improperly measured due to its low angular value.

Zeolitic water needs to be removed from the clay channels to allow for indigo accommodation. This happens when the clay is heated between 100 and 300 °C. In the prepara-

tion the temperature of the indigo/clay mixture was maintained at 105 °C for 24 hours. Therefore, it is likely that only a *partial* loss of the zeolitic water molecules had occurred. Moreover, after heating, a re-hydration process could have taken place and water molecules from environmental moisture could have entered the clay channels again. Therefore, indigo and zeolitic water compete to occupy positions inside the clay channels. The absence of the organic dye, though, does not imply the presence of water. In fact, if an indigo molecule is firmly anchored through hydrogen bonds at one end of a channel, it may act as a plug, and prevent the water molecules from entering the channel. The re-hydration process may not occur and the internal part of the channel may remain empty. On the other hand, if the dehydration is not complete due to low temperature during preparation, it seems more likely that the water molecules closer to the channel opening are preferentially removed and substituted by indigo, leaving the inner part of the channel occupied by water. Both indigo and zeolitic water were therefore considered part of the Maya Blue models, and their occupancy factors were refined.

Indigo in MB is bound to be highly disordered. In fact, in the 3-cells superstructure indigo can be affected by at least a 6-fold disorder. This is due to the fact that the flat molecule can enter the channel in two different ways (*e.g.* with the C=O group on one side or the other), the probability of the two events being equal. Once inside the channel, the molecule can no longer flip around its mayor axis, thus causing a two-fold disorder. Furthermore, each molecule can occupy three different positions, along the *Z* axis, corresponding to the formation of H-bonds with different structural water of palygorskite. This implies that indigo molecules can be *out of phase* with respect to other molecules in neighbouring cells, although this fact cannot be asserted *a priori*. The total number of combinations is therefore 6, and each possibility may or may not have the same probability.

6.1. Rietveld refinement of a 3-cells superstructure of Maya Blue

The complete set of coordinates derived by molecular modelling in this study was adopted as the starting model for MB. A 25 parameters shifted Chebishev function was used to model the background and the Simpson's rule integration of pseudo-Voigt peak profile function was adopted for all phases. The refinement was carried out trying to avoid high correlations between structurally related parameters, by fixing one of them alternatively when that occurred. In the early stages of refinement only the scale factors, the lattice parameters and the *W* coefficient (Caglioti *et al.*, 1958) for each phase were adjusted.

Due to the complexity and similarity of the MP and OP structures, which resulted on a large peaks superposition and therefore a relatively ill defined procedure, the individual atomic coordinates were not varied. The indigo molecule was refined applying *rigid body* constraints, to look for the correct orientation inside the clay channels. Only *Y* axis rotations are compatible with the lattice symmetry operators. The rotation proved not to be significant, confirming

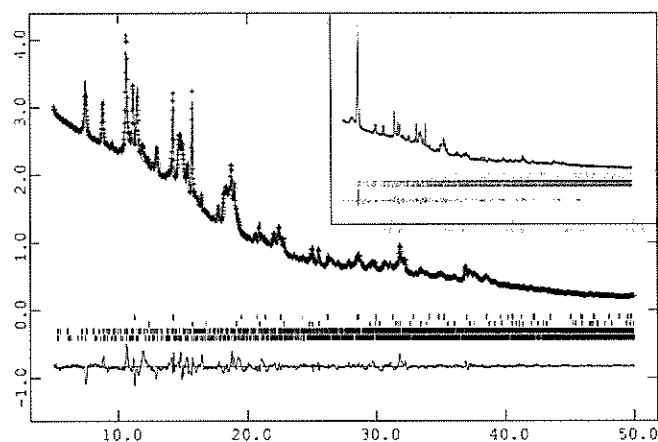


Fig. 5. Rietveld refinement profile for Maya Blue (3-cells superstructure).

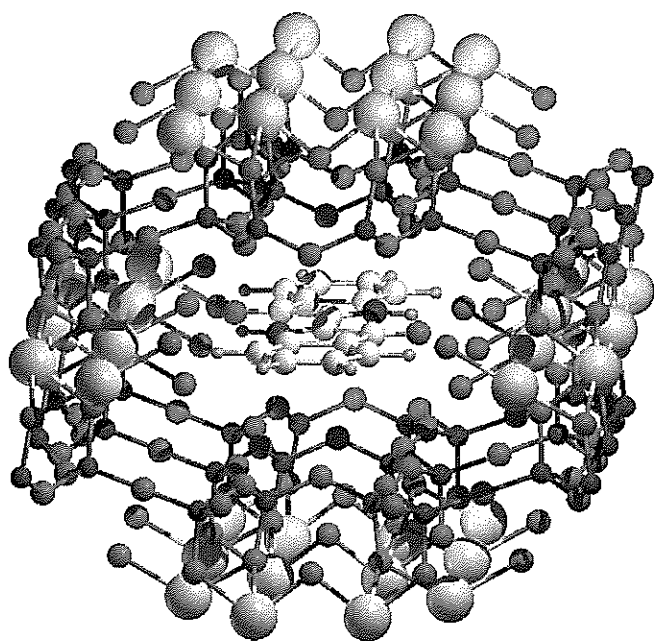


Fig. 6. Maya Blue structure, limited to one channel, projected on the (001) face.

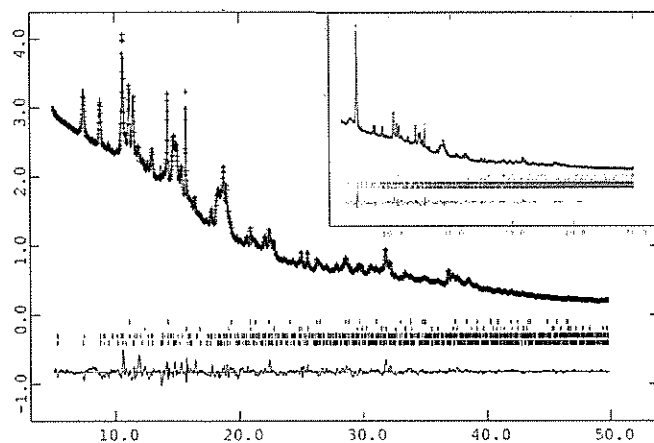


Fig. 7. Rietveld refinement profile for Maya Blue (single cell with disordered indigo).

Table 2. Rietveld refinement of the 3-cells superstructure Maya Blue. a) Formula, space group, cell parameters, and refinement data. b) Atomic coordinates for MP and OP for the 3-cell superlattice of Maya Blue.

Table 2. a

	MP (3 cells+indigo)	OP (3 cells+indigo)
Formula	$3[(\text{Mg}, \text{Al})_4\text{Si}_8(\text{O}, \text{OH}, \text{H}_2\text{O})_{24} \cdot n\text{H}_2\text{O}] + 2\text{C}_6\text{N}_2\text{O}_2$	
Space group	<i>C2/m</i>	<i>Pbmm</i>
<i>a</i> (Å)	13.410(4)	12.709(3)
<i>b</i> "	17.891(5)	17.896(5)
<i>c</i> "	15.740(4)	15.775(5)
β (°)	107.06(2)	-
<i>V</i> (Å ³)	3610(1)	3588(1)
Weight frac. (%)	46.8(6)	40.5(7)
$\Delta\rho_{\text{min}}, \Delta\rho_{\text{max}}$ (e/Å ³)	-0.76, 1.95	-0.68, 1.60
GW, L(X)	8.9(8), 13.9(7)	8.9(8), 13.9(7)

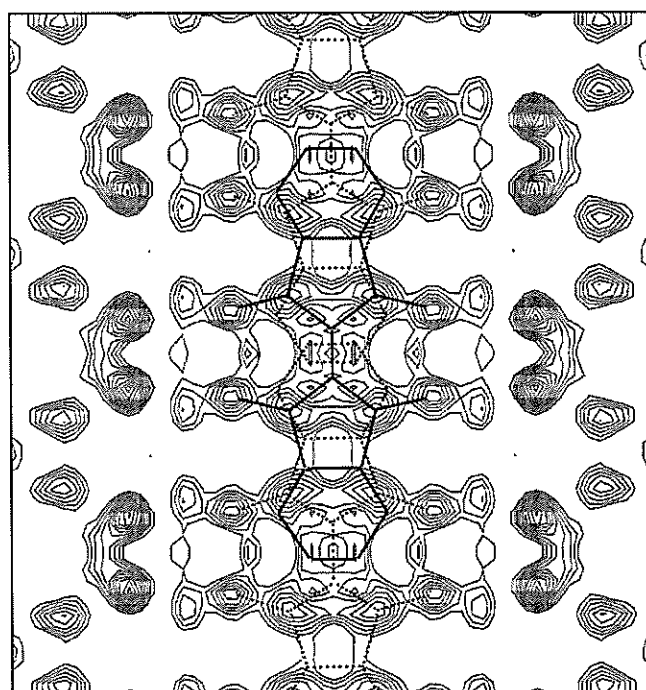


Fig. 8. Difference Fourier syntheses for OP, as calculated from the Rietveld refinement of the three-cells superstructure, after removing the indigo molecule from the model before calculation.

the indigo tendency to lay on the (100) plane, as suggested by the molecular modelling simulations.

The sum of the occupancy factors was constrained to be 1 for zeolitic water plus indigo (initially set at 0.5 each). For both palygorskite polytypes the zeolitic water occupancy increased, while that of indigo decreased. This confirms that MB is highly hydrated and that the presence of indigo in the channel is strongly subordinated to that of the zeolitic water. In particular, the indigo occupancy was slightly higher in the orthorhombic (34%) than in the monoclinic form (27%).

Table 2. b

Atom	MP (3 cells + indigo)				OP (3 cells +indigo)			
	x	y	z	Frac.	x	y	z	Frac.
Si1	0.714	0.413	0.325	1.00	0.223	0.915	0.601	1.00
Si1'	0.272	0.413	0.013	1.00	0.723	0.585	0.733	1.00
Si1''	0.714	0.413	0.659	1.00	0.223	0.915	0.934	1.00
Si2	0.705	0.333	0.494	1.00	0.218	0.835	0.437	1.00
Si2'	0.273	0.333	0.844	1.00	0.718	0.665	0.896	1.00
Si2''	0.705	0.333	0.827	1.00	0.218	0.835	0.771	1.00
Mg2	0.5	0.416	0.5	1.00	0	0.919	0.5	1.00
Mg2'	0.5	0.416	0.833	1.00	0	0.919	0.833	1.00
Mg3	0.5	0.340	0	1.00	0	0.842	0	1.00
Mg3'	0.5	0.340	0.667	1.00	0	0.842	0.667	1.00
OH	0.424	0.5	0.539	1.00	0.926	0	0.218	1.00
OH'	0.571	0.5	0.805	1.00	0.926	0	0.552	1.00
OH''	0.424	0.5	0.873	1.00	0.926	0	0.886	1.00
O1	0.587	0.410	0.287	1.00	0.095	0.912	0.595	1.00
O1'	0.399	0.410	0.050	1.00	0.595	0.588	0.739	1.00
O1''	0.587	0.410	0.621	1.00	0.095	0.912	0.928	1.00
O2	0.580	0.347	0.467	1.00	0.092	0.849	0.441	1.00
O2'	0.398	0.347	0.871	1.00	0.592	0.651	0.892	1.00
O2''	0.580	0.347	0.800	1.00	0.092	0.849	0.775	1.00
W1	0.584	0.245	0.648	1.00	0.399	0.752	0.290	1.00
W1'	0.383	0.245	0.686	1.00	0.399	0.752	0.625	1.00
W1''	0.584	0.245	0.982	1.00	0.399	0.752	0.956	1.00
O3	0.243	0.5	0.004	1.00	0.75	0	0.392	1.00
O3'	0.751	0.5	0.671	1.00	0.75	0	0	1.00
O3''	0.243	0.5	0.671	1.00	0.25	0.5	0.941	1.00
O4	0.25	0.75	0.5	1.00	0.25	0.75	0.439	1.00
O4'	0.25	0.75	0.833	1.00	0.75	0.75	0.894	1.00
O4''	=	=	=	1.00	0.25	0.75	0.773	1.00
O5	0.742	0.372	0.418	1.00	0.265	0.875	0.519	1.00
O5'	0.239	0.372	0.920	1.00	0.765	0.626	0.815	1.00
O5''	0.742	0.372	0.751	1.00	0.265	0.875	0.852	1.00
O6	0.754	0.368	0.589	1.00	0.254	0.870	0.350	1.00
O6'	0.228	0.368	0.749	1.00	0.754	0.630	0.984	1.00
O6''	0.754	0.368	0.922	1.00	0.254	0.870	0.683	1.00
ZW1	0.5	0.155	0.5	0.73(9)	0.5	0.8703	0.5	0.66(6)
ZW1'	0.5	0.155	0.833	0.73(9)	0.5	0.8703	0.8333	0.66(6)
ZW2	0.5	0.084	0	0.73(9)	0.5	0.9435	0	0.66(6)
ZW2'	0.5	0.084	0.6667	0.73(9)	0.5	0.9435	0.6667	0.66(6)
C1	0.0017	0.5	0.4549	0.27(9)	0.004	0.5	0.4546	0.34(6)
C2	0.0036	0.5747	0.4013	0.135(5)	0.0088	0.5747	0.4009	0.170(3)
C3	0.0068	0.5436	0.3140	0.27(9)	0.0165	0.5436	0.3131	0.34(6)
C4	0.0097	0.5806	0.2349	0.27(9)	0.0235	0.5806	0.2336	0.34(6)
C5	0.0124	0.5376	0.1616	0.27(9)	0.030	0.5375	0.160	0.34(6)
N1	0.0036	0.4367	0.4014	0.135(5)	0.0087	0.4367	0.401	0.170(3)
Oin	0.0029	0.6413	0.4218	0.135(5)	0.0069	0.6413	0.4214	0.170(3)

Tables 2a, 1b and 2b show the complete set of data for the refinement, and Fig. 5 shows the *observed*, *calculated* and *difference* powder diffraction patterns for the 3-cells MB. Fig. 6 shows a channel of the MB structure projected on the (001) face.

6.2. Fourier maps

Difference Fourier maps (DF) for both M and O palygorskite were calculated. There is a reasonable good fit between observed (F_o) and calculated (F_c) structure factors (minima and

maxima ranging from -0.76 and $1.95 e^{-}/\text{\AA}^3$ for monoclinic and -0.68 and $1.60 e^{-}/\text{\AA}^3$ for orthorhombic palygorskite).

The presence of indigo in the clay channels was confirmed by calculating a Difference Fourier Map after removing its molecule from the MB model. The DF map for orthorhombic palygorskite is shown in Fig. 8, with indigo outlined using dark solid lines in the position used for the refinement. The X axis of the map coincides with the b direction, while the Y axis of the map coincides with c of palygorskite. The map represents the central part of a clay channel, where the indigo molecule is located.

Two indigo atoms only, namely the oxygen and the nitro-

gen, could be reasonably well located. This way of interpreting the DF takes into consideration the two-fold disorder due to the flipping of indigo around its major axis, but not the three-fold disorder due to the three possible positions along the *Z* axis of the supercell. In order to do this, on the DF of Fig. 8, the other two indigo molecules were drawn in dotted lines. All the atoms of the three molecules lay on regions of positive electron density, even though it is still impossible to locate all of them. Positive peaks that could not be explained on the basis of one indigo molecule only (ordered MB) can now be justified. One can conclude, therefore, that the indigo molecule is completely disordered. Similar but worse results were obtained for monoclinic palygorskite.

A trial to see if the structure could be "independently solved" was performed, by introducing the located atoms and recalculating a DF in the model, but no other peaks were found.

The reason for trying to refine the MB structure using a three-cells model was that one cannot have *a priori* knowledge of the fact that one or more of the possible configurations of the six-fold disorder is not prevalent. By looking at the XRPD patterns of the clay and of MB one cannot see any peak revealing a superstructure, since this information may be confined into subtle intensity variations. On the basis of the results of the Difference Fourier map one can instead conclude that the disorder is complete. This multi-grade disorder, only partially predictable, coupled with the possibility of empty spaces or cells occupied by water, inevitably affected the goodness of the refinement, which could not be carried out varying the coordinates of each atoms. On the other hand, a full-structure analysis (varying all atoms coordinates) would have been unreliable, due to the excessive number of parameters involved. A further problem was given by the peak superposition for a multiphase refinement with highly related polymorphs (Young, 1993). Even using the high-resolution of the synchrotron radiation, no peak attributable to the 3-cells superstructure was found.

6.3. Rietveld refinement of a single-cell Maya Blue model, with disordered indigo

If the disorder of the indigo molecules is complete, the MB structure can equally well be described in terms of a single palygorskite cell, in which all indigo atoms are located correspondingly (see central palygorskite cell in Fig. 8, considering both the atoms connected by solid and dotted lines). Since three indigo molecules can alternatively occupy the channel in different positions, their occupancies were set to 1/3 per each atom (to 1/6 for O, N and C2, which do not have a corresponding atom within the indigo molecule).

The atom coordinates (both for OP and MP) were taken from the models refined in this study for pure palygorskite. The indigo coordinates were taken from the supercell refinement, setting the inversion centre of the molecule on the centre located at 0, 1/2, 1/2 in the clay lattice. The three-fold disorder is automatically taken into account by bringing the whole asymmetric part of indigo into a single clay cell.

A full-structure refinement was carried out, since the number of independent variables was reduced and the corre-

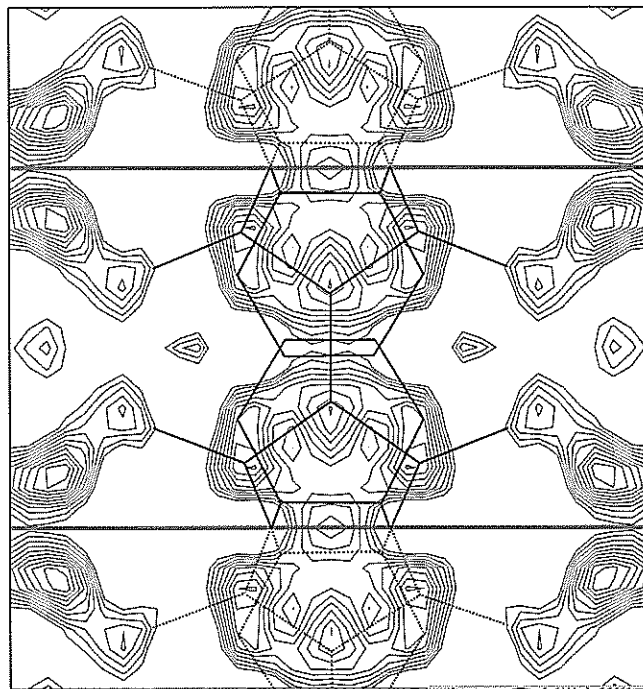


Fig. 9. Difference Fourier synthesis for OP, as calculated from the Rietveld refinement of the disordered "1-cell" structure, after removing the indigo molecule from the model.

lation among clay atoms related by pseudo-translational symmetry was eliminated.

The same conditions as the previous refinements were adopted for the treatment of the background and for the profile function of all phases. After a few runs, the atomic coordinates and the occupancy factors for all atoms were refined, under soft constraints.

The occupancy factors of zeolitic water and indigo atoms, initially set at 0.5 and 0.1667 (0.5/3) respectively, were constrained to vary so that the total sum would be equal to 1. The zeolitic water occupancy increased while that of indigo decreased. The results were coherent with those obtained in the 3-cells MB refinement. The occupancy of indigo is higher in the orthorhombic (33%) than in the monoclinic form (27%). The zeolitic water molecule labelled "ZW2" in orthorhombic palygorskite moved to the special position 0, 1/2, 0. For both polytypes the distances (≈ 2.6 Å) between the clay structural water and the C=O group of indigo are compatible with the formation of H-bonds, in agreement with the chemical modelling results.

The refinement conditions, agreement factors, cell parameters, weight percentages and atom coordinates for both palygorskite polymorphs are reported in Table 1 (a, b and c).

Fig. 7 shows the *observed*, *calculated* and *difference* powder diffraction patterns for the "one-cell" refinement of MB.

Comparing the results of the "1-cell" refinement with the "3-cells" model one can see that the first gave better agreement factors (Table 1b) and lower residuals in the DF maps (Tables 1a and 2a) as well as a slightly better agreement for the profile fit (Fig. 5 and 7). This may indicate that indigo makes a contribution to the refinement of Maya Blue, and that its distribution is disordered.

Fig. 9 shows the DF map for OP, with indigo outlined using dark solid lines inside the single cell and dotted lines outside. Four (out of seven) indigo atoms can be located. The oxygen atom position appears near a weak peak, but looking at the section at $a = 0.02$ above the plane, there is an intense peak, perfectly centred. The other two atoms cannot be located, although their expected positions lie on a region of positive electron density. Similar but worse results were obtained for monoclinic palygorskite. Introducing in the model the located atoms and recalculating a DF, no more peaks were found. According to the refined value of the occupancy factors, the amount of indigo present is less than 1/3 of the maximum possible value, corresponding to less than 2% in weight. These data support what stated by Kleber *et al.* (1967), who obtained the pigment by mixing the clay with quite small amounts of indigo. Despite the low indigo content, the pigment has a bright turquoise colour.

To eliminate the uncertainties due to the zeolitic water positions, data have already been collected on deuterated Sac l'um, using neutron diffraction. As for the definite confirmation of the indigo position, a neutron diffraction data collection on MB prepared with deuterated indigo is planned.

6.4. Relative abundance of monoclinic and orthorhombic polymorphs

Rietveld refinement allowed for the quantitative determination of the phases present in our mixture. In the case of the two polymorphs of palygorskite the results may be affected by errors larger than usual, given the strong similarity between the two structures and therefore the high superposition of peaks. Nevertheless, if one refines palygorskite samples coming from different sites, one can see that the ratio between M and O palygorskite is quite different according to the locality of provenance. Table 3 shows some of the values obtained for four localities. These include Bolca, Italy, (Perego, 1998), a Sac l'um from Ticul (Reyes-Valerio, 1993), one sample taken in a mine at Ticul, on the road Ticul Chapab, and four samples collected at several metres from one another in the Cenote Sac l'um in Ticul (Audagnotti, 2001). The sample Ticul contains only palygorskite. The samples from Bolca and Ticul-Chapab contain also a percentage of calcite, while dolomite was present in the samples taken from the cenote. These differences unfortunately can hardly be exploited for provenance determination since it is impossible to separate the MB pigment from the plaster support, which occasionally contains both calcite and dolomite.

The values for samples taken at a distance of a few metres from one another in the same outcrop (last four values in Table 3), are the same within the standard errors. Conversely there is a significant difference among the relative abundance of MP and OP in samples coming from different sites. This observation can lead, hopefully, to a method for studying the provenance of the archaeological MB samples. In fact, any sort of analysis which includes the whole specimen as taken from a mural painting or a ceramic necessarily includes part of the support, which is very likely made of local materials (lime, sand, clay *etc.*). It is of great archaeological

Table 3. Relative percent abundance of M and O palygorskite as obtained from Rietveld refinement of samples coming from different sites.

Sample	MP (%)	OP (%)
Bolca	33.1 (8)	66.9 (7)
Ticul-Chapab	59.8 (7)	40.2 (8)
Ticul	43.6 (7)	56.4 (7)
Cenote Sacalum 1	41.5 (6)	58.5 (6)
Cenote Sacalum 2	42.0 (6)	58.0 (8)
Cenote Sacalum 3	41.8 (7)	58.2 (6)
Cenote Sacalum 4	42.7 (6)	57.3 (7)

interest to determine whether MB was discovered in one place and its manufacture was kept as a precious secret in order to sell the product to other Mayan Cities or, on the contrary, the artisans of every Mayan City learned the technology and manufactured on site the pigment, possibly using locally available palygorskite. In order to do this, the determination of the ratio between the amounts of M and O palygorskite seems to be very promising, although cumbersome.

7. Concluding remarks

A theoretical model for MB structure was confirmed via energy minimisation calculations and Rietveld refinements on powder diffraction spectra, collected with synchrotron radiation. The main features of the proposed MB structure are:

a) The pigment is formed by the insertion of indigo molecules in the channels characterizing the palygorskite structure. The only other clay capable of forming a stable complex with indigo is sepiolite, which contains very similar, although double in size, channels. This process occurs at T around 100 °C, when part of the zeolitic water occupying the clay channels starts being lost. The colour of the pigment (turquoise instead of the deep dark blue of indigo) is due to the interaction of indigo with the clay. The presence of Fe nano-particles and their possible Rayleigh scattering invoked to justify the colour (Yacamán *et al.*, 1996) seems not to be necessary, since the colour of the clay is pale yellow and only when indigo is added the blue colour appears. More interesting is the hue change which takes place only after heating above 100 °C. This is likely due to the formation of hydrogen bonds, which partially localize the resonant electrons of the chromophore, changing the light adsorption band. On this subject further study is needed.

b) The insertion of indigo into palygorskite, if completely ordered, would determine a 3-cells superstructure, oriented along the Z axis. The present study demonstrates that the MB structure presents a 6-fold disorder, due to the fact that there are two possibilities for the molecule to enter the channel, and three possible positions along the Z axis, allowing the formation of H-bonds. Furthermore, there is the presence (or absence) of zeolitic water, which given the temperature of formation is not completely eliminated. This fact, coupled with the very low amount of indigo in MB (less than 2% in weight) explains why it is not possible to find in the powder diffraction pattern concluding evidence of a superstructure.

c) Of the two polymorphs of palygorskite, OP has a slightly larger content of indigo than MP. In both cases, hydrogen bonds are established between indigo and palygorskite, giving to the compound its strong stability ($H-O = 1.74 \text{ \AA}$ for MP and 1.85 \AA for OP from molecular modelling).

d) The ratio between the abundance of OP and MP in palygorskite, obtained by Rietveld refinement, varies according to the location in which the clay is found. The determination of this ratio can be applied to ancient Maya Blue specimens, in order to establish the provenance of the material.

Acknowledgements: The authors are deeply in debt with Constantino Reyes-Valerio, who for several years contributed his vast experience on the subject, together with samples of ancient Maya Blue and of the product he synthesised, used for the measurements. We would like to thank Gilberto Artioli for kindly collecting the data and the Mexican archaeologists Alejandro Martínez Muriel and Leonardo López Luján, for providing valuable information on the history of Maya Blue. We are particularly grateful to Eric Doehne of the Getty Conservation Institute for the ESEM pictures. We thank the European Synchrotron Radiation Facility of Grenoble, for the use of the equipment.

We would like to thank the referees of this paper who gave us many constructive suggestions. The CNR Target Project on Cultural heritage financed this study.

References

- Ajò, D., Favaro, M., Reyes-Valerio, C., Chiari, G., Giustetto, R. (2000): Characterisation of Maya Blue by photoluminescence spectroscopy. *Archaeometry* 2000, Mexico (in press).
- Artioli, G. & Galli, E. (1994): The crystal structures of orthorhombic and monoclinic palygorskite. *Material Science Forum*, **166**, 647-652.
- Artioli, G., Galli, E., Burattini, E., Cappuccio, G., Simeoni, S. (1994): Palygorskite from Bolca, Italy: a characterization by high-resolution synchrotron radiation powder diffraction and computer modelling. *N. Jb. Miner. Mh.*, **1994**, 217-229.
- Audagnotti, S. (2001): Studio diffrattometrico di minerali argillosi: palygorskite e Maya Blu. Undergraduate thesis, University of Turin.
- Bradley W. F. (1940): The structural scheme of attapulgit. *Amer. Mineralogist*, **25**, 405-410.
- Brauner, K. & Preisinger, A. (1956): Struktur und Entstehung des Sepioliths. *Tschermaks Mineralogische und Petrographische Mitteilungen*, **6**, 1-2.
- Brindley, G.W. (1959): X-ray and electron diffraction data for sepiolite. *Amer. Mineralogist*, **44**, 5-6.
- Cabrera, J.M. (1969): El Azul Maya. Informes y trabajos del Instituto de Conservación y Restauración de Obras de Arte, Arqueología y Etnología N° 8, Madrid.
- Caglioti, G., Paoletti, A., Ricci, F. P. (1958): Choice of collimator for a crystal spectrometer for neutron diffraction. *Nucl. Instrum. Methods*, **35**, 223-228.
- Catherwood, F. (1844): Views of Ancient Monuments in central America, Chiapas, and Yucatan. New York: Barlett and Welford.
- Chiari, G., Giustetto, R., Reyes-Valerio, C., Ricchiardi, G. (2000): Maya Blue pigment: a palygorskite-indigo complex. *Atti XXX Congresso A.I.C.*, Martina Franca, September 2000, p. 184 http://srs.dl.ac.uk/arch/posters/CHIARI/maya_bari_poster/index.htm linked from <http://srs.dl.ac.uk/arch/other-communications.html>
- Chisholm, J. E. (1990): An X-ray powder-diffraction study of palygorskite. *Canad. Mineralogist*, **28**, 329-339.
- (1992): Powder-diffraction patterns and structural models for palygorskite. *Canad. Mineralogist*, **30**, 61-73.
- De Lapparent, J. (1938): Défence de l'attapulgit. *Bull. Soc. Miner.*, **61**, 253-283.
- Effenberg, H., Mereiter, K., Zemann, J. (1981): Crystal structure refinements of Magnesite, Calcite, Rhodochrosite, Siderite, Smithonite and Dolomite with the discussion of some aspects of the stereochemistry of Calcite type carbonates. *Z. Kristallogr.*, **156**, 233-243.
- Ewald, P.P. (1921): *Ann. Phys.*, **64**, 253-287.
- Ferraris, G., Khomyakov, A.P., Belluso, E., Soboleva, S.V. (1998): Kalifersite, a new alkaline silicate from Kola Peninsula (Russia) based on a palygorskite-sepiolite polysomatic series. *Eur. J. Mineral.*, **10**, 865-874.
- Fester, G.A. (1955): Some dyes of the ancient South American Civilizations. *Isis*, **44**, 13-16.
- Gettens, R. J. (1962): Maya Blue: an unsolved problem in ancient pigments. *Amer. Antiquity*, **27**, 557-564.
- Gettens, R.J. & Stout, G.L. (1942): *Painting Materials – A short Encyclopaedia*. Van Nostrand, New York.
- Glinnemann, J., King, H. E. jr, Schulz, H., Hahn, Th., La Placa, S.J., Dacol, F. (1992): Crystal structure of the low temperature quartz type phases of SiO_2 and GeO_2 at elevated pressures. *Z. Kristallogr.*, **198**, 177-212.
- Hammersley, A.P., Svensson, S.O., Hanfland, M., Fitch, A.N., Hammersmann, D. (1996): Two-dimensional detector software: from real detector to idealised image or two-theta scan. *High Pressure Research*, **14**, 235.
- Kleber, R., Masschelein-Kleiner, L., Thissen, J. (1967): Étude et identification du "Bleu Maya". *Studies in Conservation*, **12**, 41-55.
- Kukovsky, Y.G. & Ostrovskaya, A.B. (1961): First palygorskite (attapulgit) deposit in the USSR. *Proceedings of All Union Mineralogical Society*, **90**, 598-601.
- Larson, A.C. & Von Dreele, R.B. (1986): GSAS. General Structure Analysis System. Report LAUR-86-748, Los Alamos National Laboratory, NM.
- Littmann, E.R. (1980): Maya Blue: a new perspective. *Amer. Antiquity*, **45**, 87-100.
- (1982): Maya Blue further perspectives and the possible use of indigo as the colorant. *Amer. Antiquity*, **47**, 404-408.
- Magaloni, D. (1998): El arte en el hacer: técnica pictórica y color en las pinturas de Bonampak. In: La pintura mural prehispánica en México. II Area Maya, UNAM, IIE, Directora Beatriz de la Fuente, **II**, 48-80.
- Merwin, H. E. (1931): Chemical analysis of pigments. In: Morris, E.H., Charlott, J. & Morris, A.A. "The Temple of the Warriors at Chichen Itza, Yucatan", Washington, D.C., Carnegie Institution of Washington, Publ. 406.
- Molecular Simulations, San Diego, (1996): In: Catalysis software release 4.0.0.
- Palacios-Lazcano, L. & Reyes-Valerio, C. (1993): Analisis del Azul Maya por espectroscopia de infrarrojo mediante la trasformada de Fourier. in De Bonampak al templo Mayor – El azul maya in Mesoamerica. Siglo XXI Editores. Apéndice, 143-154.
- Pascarelli, S., Boscherini, F., D'Acapito, F., Hrdy, J., Meneghini, C., Mobilio, S. (1996): X-Ray optics of a dynamical sagittal-focusing monochromator on the GILDA beamline at the ESRF. *J. Synchrotron radiation*, **3**, 147-155.

- Perego, A. (1998): Determinazione strutturale di composti di tipo palygorskite. Undergraduate thesis, University of Milan.
- Polette, L.A., Ugarte, N., Chianelli, R.R., Yacamán J.M. (2000): Decoding the chemical complexity of a remarkable ancient paint. *Discovering Archaeology*, linked at: www.discoveringarchaeology.com/0900toc/Maya%20Blue-feature.htm.
- POV-RAY freeware. Carson, C. (1996-99): Copyright of the Persistence of Vision Development Team.
- Preisinger, A. (1963): Sepiolite and related compounds: its stability and application. *Clays Clay Minerals*, **10**, 365-371.
- Reyes-Valerio, C. (1993): De Bonampak al Templo Mayor: el Azul Maya en Mesoamerica. Siglo XXI Editores.
- Roundhill, L. S., Reents-Budet, D., Mc Govern, P., Michel, R. (1989): Maya Blue: a fresh look at an old controversy. Seventh Palenque Round Table, 253-256.
- Sharer, R.G. (1994): *The Ancient Maya* (Fifth Edition). Stanford University press, 1-892.
- Shepard, A. O. & Gottlieb, H. B. (1962): Maya Blue: alternative hypothesis. in *Notes from a Ceramic Laboratory N1*, Washington, D.C., Carnegie Institution of Washington.
- Singer, A. & Galan, E. (1984): Palygorskite-sepiolite occurrences, genesis and uses. *Developments in sedimentology*, **37**, 337-343.
- Stephens, J.L. (1841): *Incidents of Travel in Central America, Chiapas, and Yucatan*. 2 Vols. New York: Harper. Reprinted by Dover (1962).
- Tagle, A.A., Paschinger, H., Richard, H., Infante, G. (1990): Maya Blue: its presence in Cuban colonial wall paintings. *Studies in Conservation*, **35**, 156-159.
- Torres Montes, L., Grinberg, A., de Grinberg, D.M.K. (1975): Distribucion geografica y cronologica del Azul Maya. XIV Reunion de Mesa Redonda de la Sociedad Mexicana de Antropologia. Honduras.
- Ugliengo, P., Viterbo, D., Chiari, G. (1993): MOLDRAW: Molecular Graphics on a Personal Computer. *Z. Kristallogr.*, **207**, 9. Available at: <http://www.ch.unito.it/ch/DipIFM/software/MOL-DRAW/MOLDRAW.html>
- Van Koningsveld, H., Jansen, J.C., Van Bekkum, H. (1987): The orthorhombic/monoclinic transition in single crystals of zeolite ZSM-5. *Zeolites*, **7**, 564-568.
- Van Olphen, H. (1966): Maya Blue: a clay-organic pigment? *Science*, **154**, 645-646.
- Virno, C. (1986): Porpora. in *La Fabbrica dei colori. Il Bagatto*. Università di Roma, 401-404.
- Yacamán, Y.M. & Serra Puche, C.M. (1995): High-resolution electron microscopy of Maya Blue paint. *Materials Research Society Symposium proceedings*, **352**, 3-11.
- Yacamán, Y.M., Rendón, L., Arenas, J., Serra Puche, C.M. (1996): Maya Blue paint: an ancient nanostructured material. *Science*, **273**, 223-225.
- Young, R.A. (1993): *The Rietveld method*. Oxford University Press.

Received 31 October 2001

Modified version received 25 March 2002

Accepted 6 August 2002



1
1
1



1
1
1

1
1
1

